Use of Numerical Weather Prediction Analysis for Testing Pressure Altitude Measurements on Aircraft - An Application Example[1]

Ulrich Schumann, Andreas Giez, Christian Mallaun, Martin Zöger and Andreas Dörnbrack

Deutsches Zentrum für Luft- und Raumfahrt, 82234 Oberpfaffenhofen, Germany

Accurate static pressure measurements are essential for safe navigation. Aircraft static pressure measurements need to be calibrated and verified. We recently compared trailing cone static pressure measurements behind two different jet aircraft up to flight level 450 during 6 flights on different days with numerical weather prediction (NWP) data. The GNSS height above mean sea level measured during these flights is compared to NWP geopotential height. The NWP data were provided by the European Centre for Medium-Range Weather Forecasts (ECMWF). The height differences at same pressure are 0.6±2.8 m on average. The corresponding pressure difference was determined to be -0.01±0.15 hPa. The method of comparing operational pressure/GNSS measurements on aircraft with NWP analysis or predictions can be used for testing the height keeping performance of aircraft after or during operation. Here we present an application example of the method. We show static pressure measured by research instruments on the German atmospheric research aircraft HALO compared to ECMWF analysis for 57 hours of data from an atmospheric research project over Europe in 2014. The method is used to derive corrected static pressure data. The corrected pressure also leads to a slightly better agreement between temperature measurements and ECMWF data which differed more when using the uncorrected pressure data as input for interpolation in the NWP data.

1 Introduction

Pressure altitude is the altitude in the ICAO standard atmosphere for given static pressure [1]. The actual atmosphere differs in temperature and density from the standard atmosphere. Hence, the pressure altitude z_p is different from the geometric altitude above mean sea level (MSL). The geometric altitude z and the horizontal position can be determined on board the aircraft using suitably processed signals of a Global Navigation Satellite System (GNSS), such as the Global Positioning System (GPS). For accurate measurement of position, differential GPS methods together with suitable post-processing are used [2]. However, without knowing the actual pressure-altitude relationship in the given atmosphere, simultaneous measurements of static pressure and geometric altitude are not sufficient to determine the accuracy of both measurements. The determination of accuracy requires an independent reference to relate static pressure to altitude.

Pressure altitude is used for aircraft navigation because it is in principle measureable on all aircraft without any reference to external systems. The pressure altitude is referenced to the standard atmosphere ground pressure setting (1013.2 hPa) and displayed to the flight crew. Static pressure is commonly measured with an appropriate pressure intake and a pressure sensor mounted at a suitably selected position on the fuselage of an aircraft. The static pressure is the pressure of the undisturbed atmosphere at rest [3] at the location of the aircraft. However, the pressure on the fuselage is disturbed by the air flow around the aircraft. Therefore, static pressure measurements need calibration corrections [4].

[1] Paper presented at Avionics & Space Testing 2017, Munich, Germany, 25/26 April

Accurate static pressure measurements are essential for safe navigation. Safe flights with reduced vertical separation minima (RVSM) require among others that the mean Altimetry System Error (ASE) under defined conditions remains below 25 m (80 ft) [5, 6], corresponding to about 3 hPa on the ground and 0.9 hPa at 11 km altitude. The ASE is the difference between the displayed pressure altitude and the pressure altitude for the static pressure in ambient air. Because of missing reference at flight, altimetry system errors are not easily detectable by the pilot or by the air traffic controllers in routine operations [6, 7]. Therefore, the height keeping performance of aircraft needs to be checked regularly. Established methods for monitoring the accuracy of altitude measurement systems are overflights of so called Height Monitoring Units (HMU), which are located on the ground, and which are capable of determining the Altimetry System Error (ASE) of individual aircraft [6]. Accurate static pressure measurements are also essential for accurate measurements of true air speed, ambient wind and ambient static temperature onboard an aircraft, and hence important for accurate airborne measurements in the field of atmospheric research.

Calibration of static pressure over the full flight envelope is usually performed during aircraft development and certification by expensive flight tests using tower fly-by maneuvers and trailing cone (TC) measurements. Recently, we developed an analysis method which can be used for static pressure calibration and for control of the height keeping performance of aircraft during operation [8, 9]. The method compares airborne pressure and geometric altitude measurements with high quality numerical weather prediction (NWP) pressure and height data. The feasibility of this approach was demonstrated by comparison of aircraft measurements taken with calibrated TC pressure sensors and differential GPS with NWP data from the Integrated Forecasting System (IFS) of the European Center for Medium-Range Weather Forecasts (ECMWF) [10]. We have shown that such high-quality NWP data are accurate enough to provide useful tests on the height keeping performance of aircraft during operation. Here, the method and the tests are summarized briefly. For illustration of the potential of the method for testing aircraft pressure-altitude data, we report an application example and experiences obtained with the German High Altitude and Long Range Research Aircraft HALO of the German Aerospace Center (Deutsches Zentrum für Luft- und Raumfahrt e.V., DLR) during the atmospheric research mission “Mid-Latitude Cirrus” (ML-CIRRUS) which was performed in March/April 2014 with HALO over parts of Europe and the North Atlantic. HALO is equipped with the Basic HALO Measurement and Sensor System (BAHAMAS) which provides accurate reference data for pressure, temperature etc. [11, 12].

A parallel study at DLR (Institute of Flight Systems, Braunschweig) investigated the same method to monitor the altitude indication of airborne aircraft air data systems on the basis of different meteorological numerical weather prediction models [13]. Within the framework of this analysis, flight experiments with the Airbus A320-232 (’Advanced Technology Research Aircraft’, ATRA) and the Dassault Falcon 20-E5 of the DLR have been conducted in order to compare the meteorological data provided by the aircraft with reference pressure measurements. Details of the NWP models used and the methods used for interpolation in the NWP data are still to be published. These two DLR studies let to a proposal for the operational use of the methodology to monitor static pressure measurements of air data systems [14], as illustrated in Figure 1.

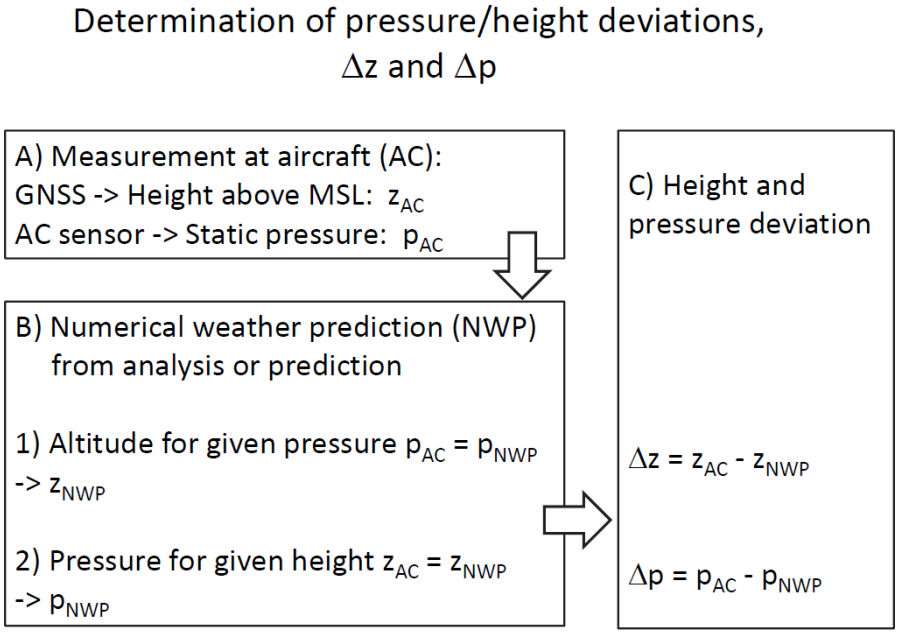

Figure 1. Use of aircraft measurements and NWP input for determination of pressure/height deviations.

2. The static pressure calibration method

The method, as outlined in Figure 1, is performed in three steps A, B and C. The method uses (A) static pressure p_{AC} and geometric altitude z_{AC} measured by the aircraft itself and (B) static pressure p_{NWP} and geometric altitude z_{NWP} data from NWP determined for the same time and horizontal position as the aircraft measurements. In step (C), the static pressure measurement error Δp is determined as the difference between p_{AC} and p_{NWP} for $z_{NWP}=z_{AC}$. Alternatively, the height error Δz can be determined as the difference between z_{AC} and z_{NWP} for same $p_{NWP}=p_{AC}$: $\Delta p= p_{TC}-p_{NWP}$ and $\Delta z=z_{TC}-z_{NWP}$.

The method may be applied as a post-processing data analysis on the ground, without expensive flight tests. The method may also be used for in-flight control of the height keeping performance of aircraft during operation. This can be done from ground or onboard the aircraft using data links to transfer the required data between aircraft and ground.

One must be careful in interpreting altitudes z_{AC}. GPS usually provides the altitude h relative to a reference ellipsoid known as World Geodetic System 1984 (WGS84)[15, 16]. The altitude z above MSL differs from the altitude h relative to WGS84, e.g., by about 50 m over the European continent. The altitude difference is known as geoid undulation N = h-z. The undulation is known and available with high spatial resolution (15“ in longitude and latitude) from the Earth Gravitational Model 1996, http://earth-info.nga.mil/GandG/wgs84/gravitymod/egm96/egm96.html.

The NWP data for the relation between p_{NWP} and z_{NWP} are obtained from the so-called „Integrated Forcasting System“ (IFS) of the European Centre for Medium-Range Weather Forecasts (ECMWF). The IFS is recognized internationally as a high-quality NWP-model for global medium range (several days) numerical weather predictions in the atmosphere at all flight levels relevant for commercial aviation. The data are available via the national weather services. Predictions are provided in regular time intervals (at least every 12 hours). For each prediction, the IFS provides global weather forecast for the coming 10 days with hourly resolution. The horizontal resolution is better than 0.25 degree in geographic latitude and longitude. Presently, K=137 vertical model layers are used. Model levels are defined in hybrid coordinates which are terrain following near the

surface and become constant pressure levels at higher altitudes [17]. The lowest model layer is bounded by the Earth surface at height z_{sfc} above mean sea level (in meter) defined with respect to the Earth geopotential (see below). The highest model layer ends at zero pressure at top of the atmosphere. In between, the pressures at model-layer interfaces are fixed functions of model layer index k=1, 2,, .., K and surface pressure p_{sfc}. For each prediction time and model-layer, the output of the IFS contains the surface pressure p_{sfc} in Pascal. Moreover, the IFS output includes the three-dimensional fields of air temperature T in Kelvin and mass specific humidity q in g/g. From this output, the vertical profiles of pressure, temperature, and humidity can be computed for each aircraft position in horizontal coordinates and time by proper numerical interpolation. Since pressure decreases about exponentially with height, it is important for numerical accuracy to interpolate in the logarithm of pressure. Otherwise one may interpolate linearly in space and time. The local air density ρ follows from the equation of state for humid air,

$$\rho = \frac{p}{R_{dry} T_V} \text{ with } T_v = T(1+\varepsilon q) \text{ und } \varepsilon = R_{dry} / R_{H2O} - 1 \quad (1)$$

Here, T_v is the so-called virtual temperature, i.e., the temperature for which the ideal gas law for dry air gives the correct density for humid air. R_{dry} and R_{H2O} are the gas constants for dry air and water vapor. The geopotential Φ is defined as an integral of Earth acceleration g over the altitude z above MSL. Observed gravity varies due to the distance to Earth's center, Earth's rotation and local gravity anomalies from crust density variations[18], so that g depends on height and geographical position. Hence we have to integrate vertically taking into account that g is a function of height, g(z):

$$\Phi = \int_0^z g(z')dz' \quad (2)$$

For constant g, Φ = g z. For an analytical function g(z), Φ can be computed analytically as well. For a more general, e.g., tabulated function g(z), Φ(z) can be computed by numerical integration. The inverse function, z(Φ), i.e. the height for given geopotential, follows analytically or numerically, possibly using a Newton-Iteration. For evaluation of Φ one has to integrate over height z. Since the model uses pressure coordinates, one uses the hydrostatic relationship

$$dp = -\rho g dz \quad (3)$$

to relate height changes dz to pressure changes dp for given density and g(z). So, for any pressure value p, one obtains the geopotential Φ(p) by numerical integration of

$$\Phi = \int_{p_{sfc}}^{p} -\frac{R_{dry} T_V}{p} dp \quad (4)$$

Hence, for any position in latitude and longitude and for any time within the prediction time period, the method provides the height z_{NWP} for a given pressure p_{NWP} and the pressure p_{NWP} for a given height z_{NWP}.

The IFS, as most meteorological global models, assumes the spherical geopotential approximation, i.e. a spherical shape of the Earth and its geopotential field with a horizontally uniform gravity field [19, 20]. Hence, the IFS assumes a constant gravity value equal to the standard gravity $g_s = 9.80665$ m s^{-2}, recommended by WMO [21]. By use of geopotential one corrects for the deviation of the local Earth surface distance from the center of Earth [22]. A variation of g with altitude is still consistent with the spherical approximation. Variable gravity is used in IFS when assimilating radio occultation data [23, 24], which comes from measurements of

GNSS signal bending angles as a function of altitude, partially in the middle atmosphere. We found that it is important for accuracy to evaluate the geopotential height with an height-latitude and possibly longitude (z,φ,λ) dependent gravity model $g=\gamma_z(z,\varphi)+\Delta g(\varphi,\lambda)$.

Other meteorological forecast models may be used for this purpose as well [25]. The various models differ in the coordinate systems used for discretization of the model equations. In particular, some models are based on model levels defined with respect to geopotential altitude and compute the pressure either hydrostatically for given air mass and gravity or by solving a Helmholtz equation for the pressure such that the continuity equations is satisfied at all positions in the computational domain for prescribed vertical velocity at the boundaries, mostly assuming constant gravity. The various discretization methods may require different interpolation methods.

3. Trailing cone tests

The pressure and altitude data of aircraft were obtained using a TC system on each of the two different jet aircraft, the research aircraft FALCON (the Dassault Falcon 20-E5) and HALO (a Gulfstream G550) operated by DLR from the airfield EDMO in Oberpfaffenhofen, Germany, see Figure 2. Both aircraft are twin-engine jets with modifications for airborne research [11].

Static pressure is measured using a dragged semi-rigid plastic hose connected to a pressure port in the undisturbed atmosphere behind the aircraft and a pressure sensor in the aircraft fuselage [26, 27]. The TC pressure is measured by high-quality pressure sensors, calibrated against a pressure reference traceable to national standards. The pressure signals are recorded along with other data in data acquisition and processing systems onboard the aircraft.

Figure 2. The aircraft HALO (top) and FALCON (bottom) with trailing cones (TC).

The height of the aircraft during TC measurements is determined with a combined DGPS and inertial measurement unit onboard the aircraft. Specifically we use an AEROcontrol-IIe system of the company IGI, http://www.igi.eu/aerocontrol.html [28]. For most of the flights, the data are post-processed with final position accuracy better than 0.1 m in the vertical (1 m without postprocessing). Postprocessing of the GNSS data with the GrafNav Software uses two-way Kalman filters based on an error model for the sensors and precise satellite

position and atmospheric correction data which are becoming available 2-3 days after the measurements. Together with the linear and rotational acceleration measurements by the inertial navigation unit, and precise position and alignment data for the various sensors, it is possible to achieve such accuracies in position and altitude [2]. The post-processing software AEROoffice used is available from the company IGI.

The TC measurements were tested using tower flyby maneuvers. TC measurements have been performed during 6 flights. The absolute accuracy of the TC pressure measurements is 0.12 hPa for HALO and 0.5 hPa for the FALCON. On the ground, this corresponds to height accuracies of 1 to 4 m.

Figure 3 shows the results for Δz (open symbols) from 159 measurements for the two aircraft (HALO and FALCON) at the 6 different measurement days versus flight level, with geopotential altitude computed from ECMWF-IFS data for variable gravity g. The full symbol with error bar depicts the mean ± 3 standard deviations on average over all Δz values. The individual data points stay well within the ±25 m (80 ft) limit and the 3-σ-error bar within the ±60 m (200 ft) limits of present RVSM requirements [5]. Hence, the data are useful to monitor altimetry system error requirements.

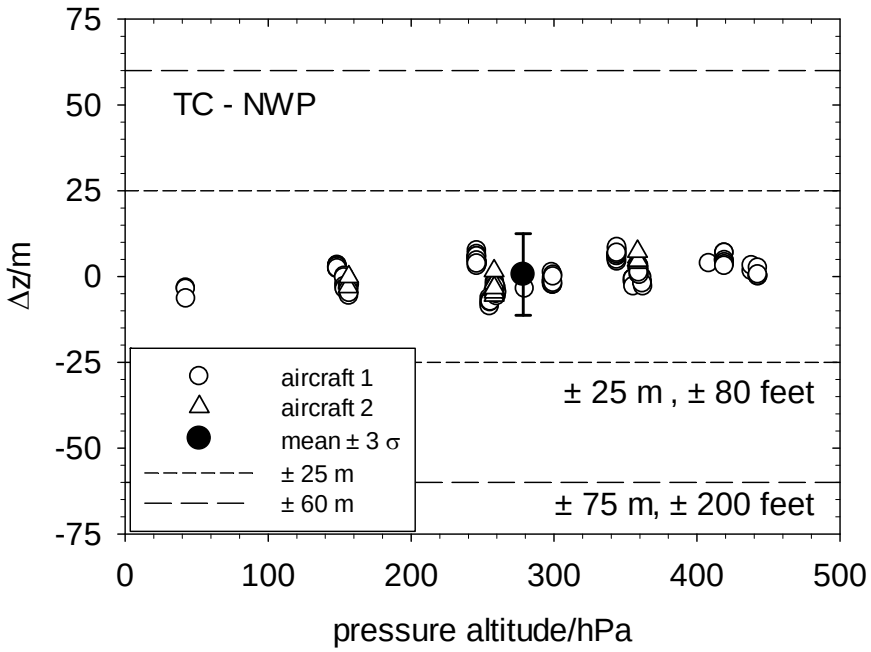

Figure 3. Height differences between TC and NWP data (analysis for variable g) versus pressure altitude in hectofeet compared to RVSM-related limits.

The accuracy of the position determination by the use of GNSS plays a significant role in computing the static pressure from NWP models. To achieve the highest degree of accuracy, post-processing the GNSS data is highly recommended, as noted also elsewhere [13].

4. Applications to HALO-BAHAMAS during ML-CIRRUS

The ML-CIRRUS experiment used measurements with the new German research aircraft HALO together with satellites observations and model analysis to gain new insights into the formation, properties, life cycle, predictability, and climate impact of natural cirrus and contrail cirrus [12]. HALO was equipped with a large set of instruments including BAHAMAS. BAHAMAS serves to measure and collect meteorological and aircraft

state parameters including static pressure, temperature and wind. The scientific payload has a mass of about 3 tons. Instruments are preferably mounted in the forward part of the aircraft within the limits of permitted range of center of gravity. The measurement system used several windows and inlets at the fuselage and underwing mounted instruments for remote sensing and for in-situ measurements.

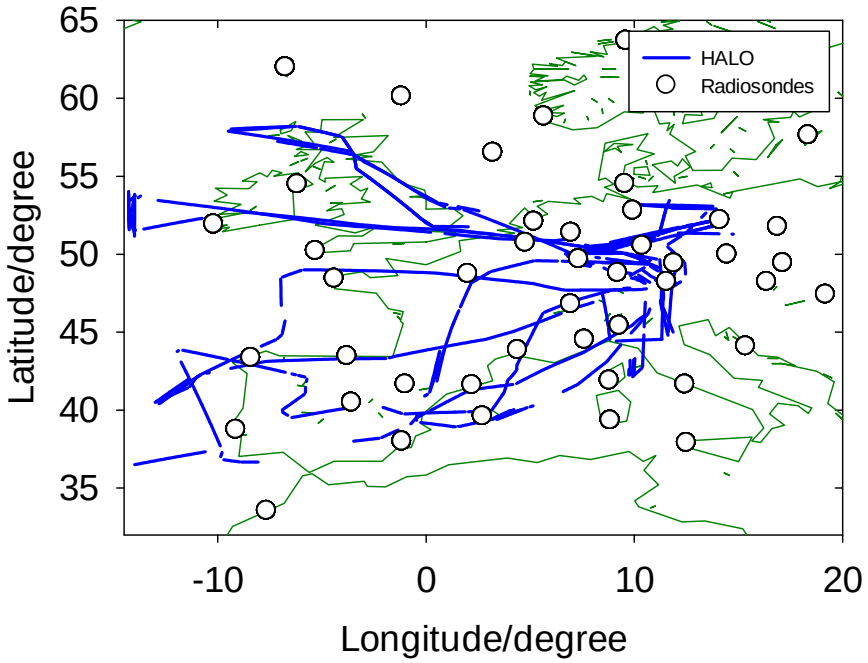

Figure 4. ML-CIRRUS HALO flight tracks used for analysis (blue) and position of radiosonde soundings used for comparisons (open circles) over a coastline map (dark green lines).

ML-CIRRUS included a total of 16 flights, with 3 preliminary test flights, and 13 scientific mission flights. Here we analyze the BAHAMAS 1-Hz data above flight level 210 from the scientific missions, with about 56 h flight time. The flights were performed at flight levels up to 450 over Europe and the Atlantic in the domain 15°W to 15°E and 36°N to 59°N in March/April 2014, see Figure 4. A preliminary comparison of static pressure from BAHAMAS with the static pressure from the Gulfstream G550 air data system showed that the BAHAMAS pressure was slightly lower than the air data pressure, with differences increasing with height. During ML-CIRRUS, the BAHAMAS pressure sensor showed some high frequency noise at about 0.31 Hz, which originate from a weak instability of the active temperature control of the main pressure sensor element. This sensor problem got fixed after the ML-CIRRUS campaign. The sensor oscillation was assumed not to affect the mean pressure values. Here we use 10-s mean values (0.1 Hz data) for comparison between HALO and ECMWF data to smooth out this oscillation. Since the BAHAMAS pressure was calibrated by the TC data described above, it was assumed that the BAHAMAS values are the more reliable ones.

Using the measured pressure for interpolation in ECMWF data it was found that the HALO temperature was about 0.6 K higher than the ECMWF temperature, see Table 1. Differences of the order 1 K are not uncommon in comparison between airborne (and satellite derived) temperature measurements and NWP data [29-31]. Even an apparently small difference is of relevance when computing relative humidity for measured absolute humidity. Relative humidity is essential for cloud formation. At a temperature of -60°C, a 0.5 K temperature overestimate causes a 7 % underestimate of relative humidity at ice saturation. Since temperature changes with

pressure altitude, a mean pressure bias could also contribute to a mean temperature bias. Of course, without further investigation, it is not clear whether any difference between HALO and ECMWF data is caused by a bias in the ECMWF data or a bias in the HALO data.

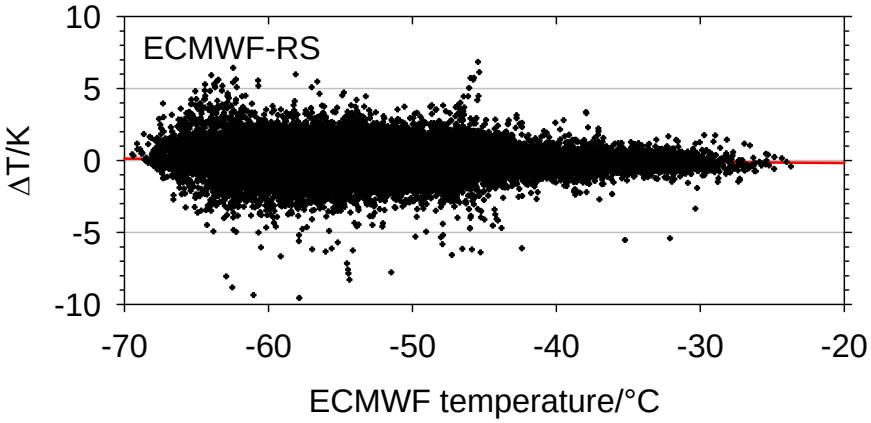

Figure 5. Temperature difference between radiosonde data and ECMWF IFS data versus IFS temperature for ML-CIRRUS.

Table 1: Differences between HALO measured and ECMWF computed values, without and with pressure correction

Variable	uncorrected		corrected	
	mean	stddev	mean	stddev
pressure/hPa	-1.39	0.56	-0.02	0.54
height/m	-40.8	19.5	-0.8	14.2
temperature/K	0.65	0.80	0.56	0.79
wind speed/(m s^{-1})	0.40	2.36	0.38	2.40
wind direction/degree	-1.0	13.9	-0.9	13.9

The ECMWF data were compared with a large set of radiosonde data. For this purpose, we collected data from 47 different radiosonde stations, distributed over the ML-CIRRUS domain in Europe, see Figure 4. The data were downloaded from http://weather.uwyo.edu/upperair/sounding.html . We found 1613 radiosoundings during the 21 days period from 26 March to 15 April 2014, with a total of 33011 measurement data in the pressure altitude range of interest (~500 to 170 hPa). For each radiosonde position, time, and pressure level, corresponding data are interpolated from NWP. The differences are plotted versus temperature in Figure 5. The mean difference between the ECMWF data and the radiosonde data is 0.03±1.1 K, without a mean trend. So the bias is practically zero. The standard deviation of about 1 K is to be expected because the local temperature measured by radiosondes must differ from the grid cell mean values represented in the NWP model which does not resolve mesoscale features such as local turbulence and gravity waves. The good agreement with the radiosonde data is a result of the four-dimensional variational data assimilation scheme used by ECMWF. We have no definite error estimate for the radiosondes used during ML-CIRRUS. For the temperature sensor of the RS92 radiosonde, with an operating range from -90°C to +60°C, the company Vaisala quotes an accuracy of better than 0.5 K [32]. This includes random errors; systematic errors are smaller [32]. The accuracy in the

troposphere (and below 16 km) could be better than 0.2 K [33-35]. Radiosonde air temperature measurements are commonly corrected for any bias from solar radiation. Here, we find no difference between day and night time data, so that any Radiosonde-IFS difference is not explained by insufficient radiation error corrections.

The agreement between the TC pressure measurements described above and the ECMWF analysis for the six flights in 2010 and 2011 implies a mean temperature bias of the IFS data of less than 0.1 K [8]. Hence, we cannot definitely conclude that the ECMWF data can serve as a reference for testing airborne temperature measurement accuracy.

These findings triggered the investigation of the pressure calibration by comparing the TC measured pressure with ECMWF pressure as described above. The comparison confirmed the high accuracies of the TC calibration and the ECMWF data, at least for the six flights in 2010 and 2011. Therefore, we now apply the comparison method to assess the accuracy of the BAHAMAS pressure data during the ML-CIRRUS flights in 2014.

The NWP data used for analysis of ML-CIRRUS data were provided by the IFS Version 40r1 http://old.ecmwf.int/research/ifsdocs/CY40r1/. The data are a combination of analysis data at 0 and 12 UTC with hourly data from forecast started from the analysis. The data set used covers the region of 60°W to 20°E, and 20°N to 70°N. The vertical pressure resolution varies between 18 hPa at the model bottom and 7 hPa at the top, corresponding to about 300 m height/10 hPa pressure resolutions near 11.5 km or 200 hPa altitudes. The spatial resolution of the data used is 0.5 degree. Higher resolution would be available from IFS but this makes no sense when using hourly time resolution. The data are interpolated linearly to the HALO aircraft position for given longitude/latitude position and time. Vertical interpolation is performed in the logarithm of pressure fields based on the static pressure measured by HALO-BAHAMAS. In order to avoid artefacts from ascending or descending flight segments, we restrict the data analysis to horizontal flight segments. For constant level legs, the deviations are slightly smaller than when including all data, though the mean values are basically unchanged.

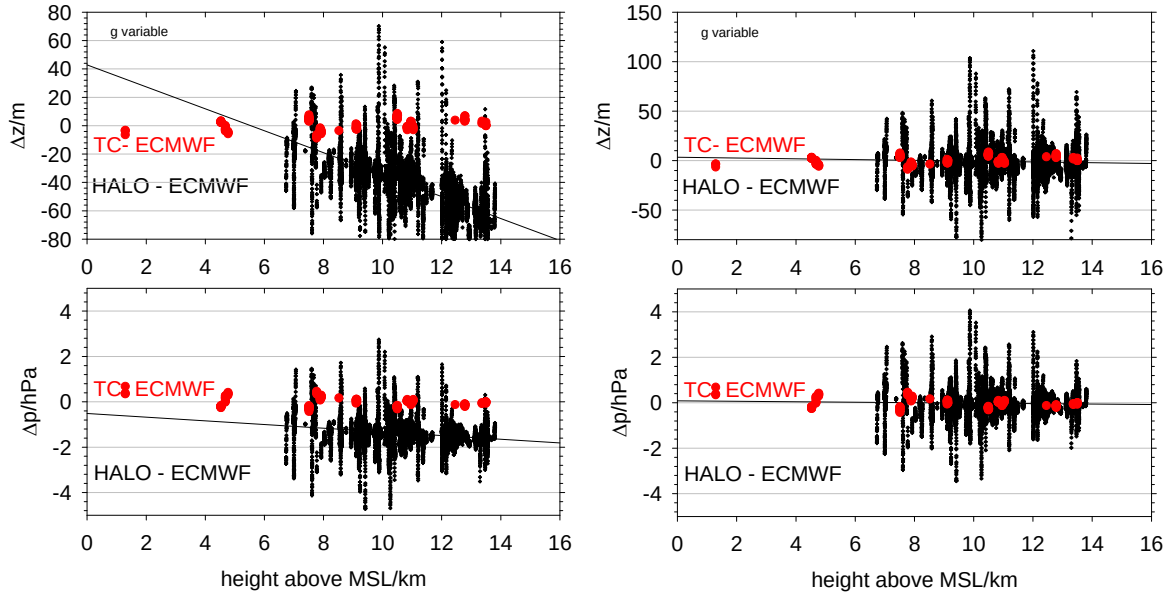

Figure 6. Left: Height and pressure differences between HALO and ECMWF data versus height above MSL for the uncorrected data (black symbols). The red symbols are corresponding TC data showing small differences between TC and ECMWF. Right, HALO-ECMWF differences after applying the pressure correction to the HALO pressure.

Figure 6 shows the height and pressure differences versus height. Compared to the TC results (red symbols), the ML-CIRRUS results exhibit far larger variability, partly because of local deviations from hydrostatic equilibrium for variable weather conditions, with clouds, gravity waves and some turbulence. We find systematic differences of the order of 40±20 m and -1.4±0.6 hPa.

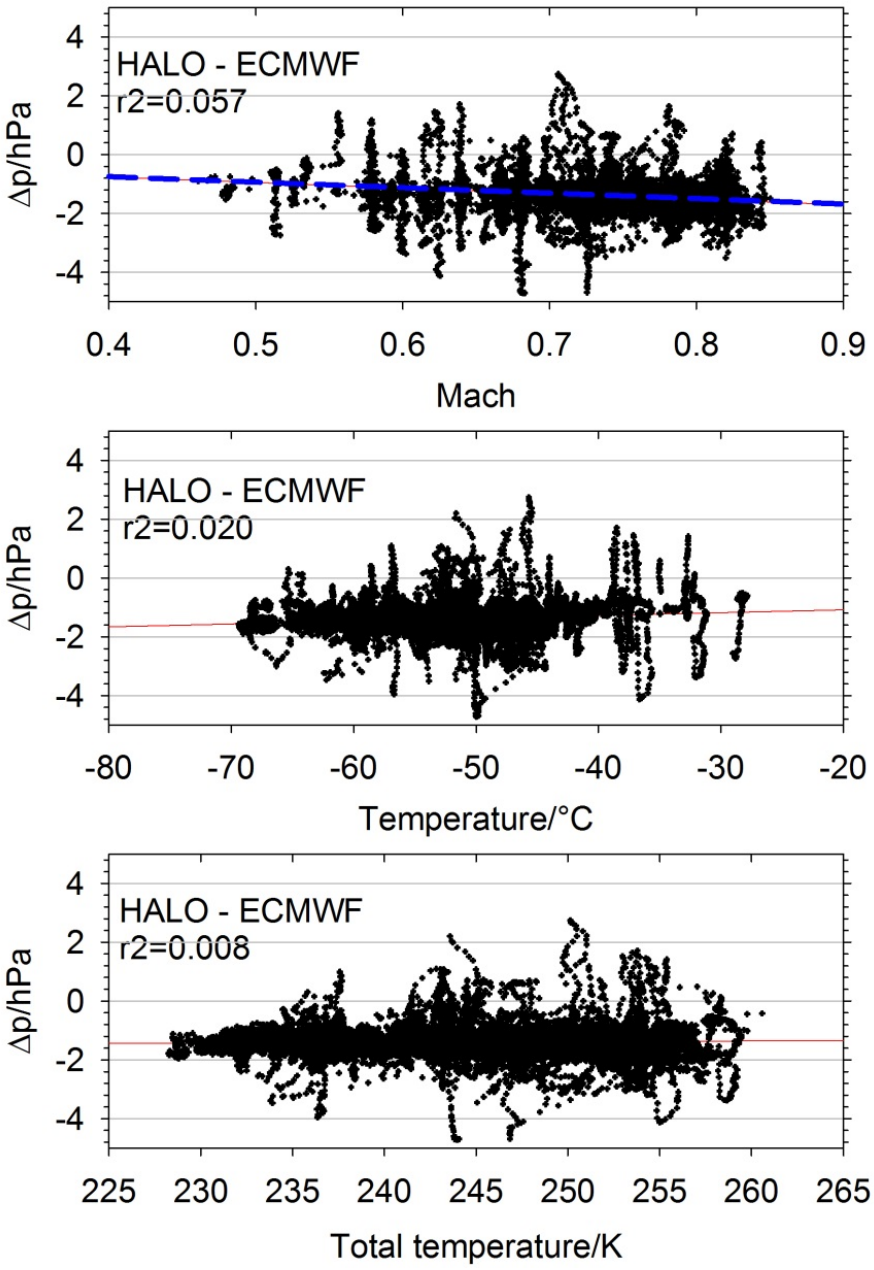

Figure 7. Pressure difference Δp between HALO-BAHAMAS static pressure versus, from top to bottom, Mach number, static BAHAMAS temperature and total BAHAMAS temperature. The red lines depict linear regressions. The quadratic correlation coefficient r^2 is given in the legends. The dashed blue line in the top panel depicts Δp/hPa = -1.865 × Ma.

The mean deviations may result partly from the fact that the static pressure calibration of the BAHAMAS pressure sensor, as derived from the previous TC measurements, is not perfectly valid for the ML-CIRRUS configuration. The changes of the HALO aircraft configuration between the TC measurements and the ML-

CIRRUS flights, with different mass loading (center of gravity) and with additional underwing mounted sensors for ML-CIRRUS, and corresponding changes in aerodynamics affecting static pressure distribution around the fuselage may explain some changes in static pressure measurements. However, instrument artefacts may also have contributed to the systematic differences.

Figure 7 shows the pressure differences as a function of Mach number, static temperature, and total temperature. The data suggest a correlation between the static pressure difference and the Mach number Ma. The value of Ma is computed from the BAHAMAS data for true air speed and temperature. The linear regression

Δp_C/hPa= 1.865 × Ma

gives corrected static pressure values p:=p+Δp_C, for which Δz and Δp are close to zero on average over all data, see Figure 6 (right). We also tested corrections as a function of static and of total temperature, but the variance of the remaining differences becomes a minimum when correcting as a function of Mach number. A correlation with static temperature would be easier to understand since any error in the sensor temperature control is likely temperature dependent. Further, we tested for any correlation of the pressure deviation with pitch angle, flight time (with changing aircraft weight), and with longitude and latitude (different gravity anomalies), but found no systematic correlations of Δp with these parameters.

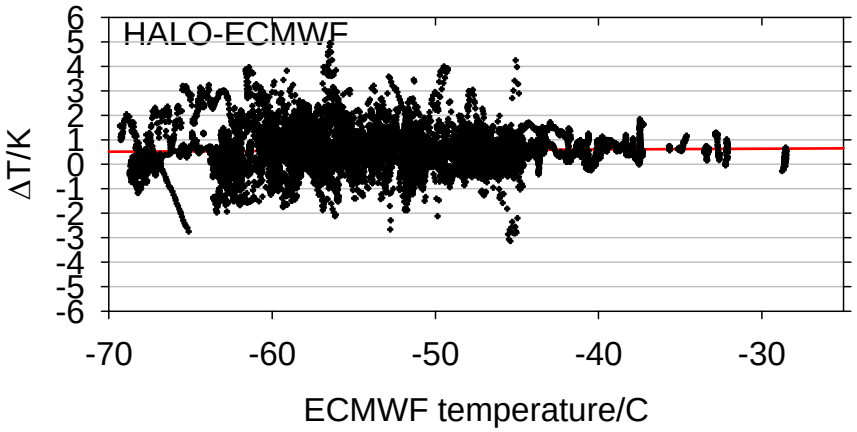

Figure 8. Temperature difference between HALO-BAHAMAS static temperature and ECMWF IFS derived temperature by interpolating with corrected pressure versus IFS temperature for ML-CIRRUS.

Figure 8 shows the differences between HALO-BAHAMAS temperature and ECMWF IFS temperature when interpolated with the corrected pressure. The red linear regression line is close to constant. Table 1 lists the mean and standard deviation of the difference between HALO measured and ECMWF analyzed variables (pressure for same height, height for same pressure, temperature, wind speed and wind direction for same pressure). We note that these wind data were determined before static pressure changes. We see that the correction successfully brings the pressure and height differences to zero mean bias and slightly smaller standard deviations. The correction also slightly reduces the temperature bias from 0.65 K to 0.56 K. The remaining bias is independent of ambient temperature. The uncorrected HALO-ECMWF temperature differences showed a weak correlation with true air speed, which is absent in the corrected version. However, the main part of the temperature bias remains unexplained. The wind speed and wind direction data are insensitive to this correction. A systematic wind deviation of 0.4 m s^{-1} is within the range of accuracy that can be expected for the BAHAMAS instrument. The systematic temperature difference calls for further investigation.

5. Conclusions

We summarized the static pressure calibration method using numerical weather prediction data as introduced before [8]. The method was tested for aircraft measurements with absolutely calibrated TC pressure sensors and differential GPS (GNSS) altitude measurements. The NWP data are based on ECMWF IFS forecast and analysis of temperature, humidity and surface pressure, including assimilated observations. The NWP data were found to be surprisingly accurate. The height differences at same pressure were found to be 0.6±2.8 m (from the sum over 6 flights with 2 aircraft). The corresponding pressure difference was determined to be -0.01±0.15 hPa. These differences are significantly below the limits required for flights with 305 m (1000 ft) vertical separation. Hence, the NWP data are accurate enough for testing static pressure measurements on aircraft.

In this paper, we describe experiences as obtained in applying the method to compute differences between the static pressure measured with BAHAMAS and the ECMWF NWP pressure for same altitudes. We showed static pressure measured by BAHAMAS on HALO compared to ECMWF analysis for 56 hours of data from an atmospheric research project with HALO over Europe in 2014. The analyses showed HALO-NWP pressure differences with large variability from day to day, partly because of variable weather conditions, with precipitating clouds, gravity waves and some turbulence. For low turbulence, the deviations are smaller, but systematic differences of the order of 40 m and -1 hPa remain. Parts of the differences may result from static pressure deviations caused by underwing mounted sensors or changed mass loading, and parts may be caused by instrumental artifacts in these flights, which are caused by a residual temperature sensitivity of the experimental pressure sensors which were used during this project. Today, HALO deploys a significantly improved version of these sensors. Anyway, the method allows deriving corrected static pressure data. The corrected pressure also leads to a slightly better agreement between temperature measurements and ECMWF data which differed more when using the uncorrected pressure data as input for interpolation in the NWP data. This study illustrates the potential of the method for testing aircraft pressure-altitude data.

References

[1] ICAO, "Manual of the ICAO Standard Atmosphere," ICAO Document No. 7488, 2nd Edition, 1964.

[2] Groves, P.D., *Principles of GNSS, Inertial, and Multisensor Integrated Navigation Systems*, ARTECH House, Boston and London, 2008, pp. 518.

[3] Anderson, J.D., *Fundamentals of Aerodynamics*, McGraw Hill, New Delhi, 2010, pp.

[4] Bange, J., Esposito, M., Lenschow, D.H., Brown, R.A., Dreiling, V., Giez, A., Marth, L., Malinowski, S.P., Rodi, A.R., Shaw, R.A., Siebert, H., Smit, H., and Zöger, M., Measurements of aircraft state and thermodynamic and dynamic variables, in *Airborne Measurements for Environmental Research*, M. Wendisch and J.-L. Brenguier, Editors, Wiley, Weilheim, 2013, p. 7-75.

[5] JAA, "Guidance Material on the Approval of Aircraft and Operators for Flight in Airspace above Flight Level 290 where a 300 m (1,000 ft) Vertical Separation Minimum is applied," Joint Aviation Authorities, Temporary Guidance Leaflet No 6 Rev 1, http://www.icao.int/ESAF/Documents/RVSM/jaa_tgl6.pdf, 1999.

[6] Eurocontrol, "Guidance Material for the Certification and Operation of State Aircraft in European RVSM Airspace," Edition: 1.0, Edition Date: 19 September 2012, https://www.eurocontrol.int/sites/default/files/article/content/documents/official-documents/guidance/2012-cmac-rma-military-guidance.pdf, 2012.

[7] Falk, C., Gonzalez, J., and Perez, J., "Using automatic dependent surveillance-broadcast data for monitoring aircraft altimetry system error," in *AIAA Guidance, Navigation, and Control Conference, 2 - 5 August, Toronto, Ontario Canada, AIAA 2010-8165*, 2010, pp. 12.

[8] Giez, A., Mallaun, C., Zöger, M., Dörnbrack, A., and Schumann, U., "Static pressure from aircraft trailing-cone measurements and numerical weather-prediction analysis," *J. Aircraft*, Vol. online, 2017, doi: 10.2514/1.C034084.
[9] Giez, A., Mallaun, C., Zöger, M., Dörnbrack, A., and Schumann, U., "Comparison of Static Pressure from Aircraft Trailing Cone Measurements and Numerical Weather Prediction Analysis," in *32nd AIAA Aerodynamic Measurement Technology and Ground Testing Conference, Washington DC, June 13-17, AIAA-2016-3707*, 2016, pp. 18, doi: 10.2514/6.2016-3707.
[10] Bauer, P., Thorpe, A., and Brunet, G., "The quiet revolution of numerical weather prediction," *Nature*, Vol. 525, No. 7567, 2015, pp. 47-55, doi: 10.1038/nature14956.
[11] Krautstrunk, M. and Giez, A., The transition from FALCON to HALO era airborne atmospheric research, in *Atmospheric Physics - Background - Methods - Trends*, U. Schumann, Editor, Springer, Heidelberg, 2012, p. 609-624, doi: 10.1007/978-3-642-30183-4_37.
[12] Voigt, C., Schumann, U., Minikin, A., Abdelmonem, A., Afchine, A., Borrmann, S., Boettcher, M., Buchholz, B., Bugliaro, L., Costa, A., Curtius, J., Dollner, M., Dörnbrack, A., Dreiling, V., Ebert, V., Ehrlich, A., Fix, A., Forster, L., Frank, F., Fütterer, D., Giez, A., Graf, K., Grooß, J.-U., Groß, S., Heimerl, K., Heinold, B., Hüneke, T., Järvinen, E., Jurkat, T., Kaufmann, S., Kenntner, M., Klingebiel, M., Klimach, T., Kohl, R., Krämer, M., Krisna, T.C., Luebke, A., Mayer, B., Mertes, S., Molleker, S., Petzold, A., Pfeilsticker, K., Port, M., Rapp, M., Reutter, P., Rolf, C., Rose, D., Sauer, D., Schäfler, A., Schlage, R., Schnaiter, M., Schneider, J., Spelten, N., Spichtinger, P., Stock, P., Walser, A., Weigel, R., Weinzierl, B., Wendisch, M., Werner, F., Wernli, H., Wirth, M., Zahn, A., Ziereis, H., and Zöger, M., "ML-CIRRUS - The airborne experiment on natural cirrus and contrail cirrus with the high-altitude long-range research aircraft HALO," *Bull. Amer. Meteorol. Soc.*, Vol. 98, No. 2, 2017, pp. 271-288, doi: 10.1175/BAMS-D-15-00213.1.
[13] Christmann, C. and Sommer, M., "Comparison of Various Numerical Weather Prediction Models for Monitoring of In-Flight Static Pressure Measurement," in *Deutscher Luft- und Raumfahrtkongress 2016, Braunschweig, 13-17 September, Bonn: Deutsche Gesellschaft für Luft- und Raumfahrt - Lilienthal-Oberth e.V. (DGLR)*, 2016, pp. 9, urn:nbn:de:101:1-201611041938.
[14] Schumann, U., Christmann, C., and Giez, A., "Verfahren und Vorrichtung zur Bestimmung eines Fehlers eines an Bord eines Fluggeräts angeordneten barometrischen Druckmesssystems," Deutsches Patentamt, submitted, 2016.
[15] Moritz, H., "Geodetic reference system 1980," *Bulletin Geodesique*, Vol. 74, No. 1, 1988, pp. 128-133.
[16] NIMA, "Department of Defense World Geodetic System 1984, Its Definition and Relationships with Local Geodetic Systems," Tech. Rep. TR8350.2, National Imagery and Mapping Agency (NIMA), 2000, pp. 175, http://earth-info.nga.mil/GandG/publications/tr8350.2/wgs84fin.pdf.
[17] Simmons, A. and Burridge, D.M., "An energy and angular-momentum conserving vertical finite-difference scheme and hybrid vertical coordinate," *Mon. Wea. Rev.*, Vol. 109, No. 4, 1981, pp. 758-766.
[18] Pavlis, N.K., Holmes, S.A., Kenyon, S.C., and Factor, J.K., "The development and evaluation of the Earth Gravitational Model 2008 (EGM2008)," *J. Geophys. Res.*, Vol. 117, No. B4, 2012, pp. B04406, doi: 10.1029/2011JB008916.
[19] Bénard, P., "An oblate-spheroid geopotential approximation for global meteorology," *Q. J. R. Meteorol. Soc.*, Vol. 140, No. 678, 2014, pp. 170–184, doi: 10.1002/qj.2141.
[20] Staniforth, A., "Spheroidal and spherical geopotential approximations," *Q. J. R. Meteorol. Soc.*, Vol. 140B, No. 685, 2014 pp. 2685-2692, doi: 10.1002/qj.2324.
[21] World Meteorological Organization, "General Meteorological Standards and Recommended Practices," Technical Regulations, Volume I, Appendix A (WMO-No. 49), Geneva., 2012.
[22] Gill, A.E., *Atmosphere–ocean dynamics*, Academic Press, London, 1982, pp. 650.
[23] Healy, S.B., "Surface pressure information retrieved from GPS radio occultation measurements," *Q. J. R. Meteorol. Soc.*, Vol. 139B, No. 677, 2013, pp. 2108-2118, doi: 10.1002/qj.2090.
[24] Aparicio, J.M. and Laroche, S., "Estimation of the added value of the absolute calibration of GPS radio occultation data for numerical weather prediction," *Mon. Wea. Rev.*, Vol. 143, No. 4, 2015, pp. 1259-1274, doi: 10.1175/MWR-D-14-00153.1.
[25] Sommer, M., "Evaluation eines Verfahrens zur Überwachung von Luftdatensystemen mit Hilfe numerischer Modelle der Atmosphäre," Master Thesis, Institut für Flugsystemtechnik, DLR Braunschweig, IB 111-2015/19, 2015, pp. 84.
[26] DeLeo, R.V. and Hagen, F.W., "Flight calibration of aircraft static pressure systems," Armed Services Technical Information Agency Publication AD 650146, http://www.dtic.mil/dtic/tr/fulltext/u2/650146.pdf, 1966, pp. 200.

[27] Giez, A., Zöger, M., and Dreiling, V. "Effective test and calibration of a trailing cone system on the Atmospheric Research aircraft HALO," *Proceedings of the 56th Annual Symposium of the Society of Experimental Test Pilots*. 2012. Society of Experimental Test Pilots, Lancaster, CA.

[28] Mallaun, C., Giez, A., and Baumann, R., "Calibration of 3-D wind measurements on a single engine research aircraft " *Atmos. Meas. Tech.*, Vol. 8, No. 8, 2015, pp. 3177-3196, doi: 10.5194/amt-8-3177-2015.

[29] Dyroff, C., Zahn, A., Christner, E., Forbes, R.M., Tompkins, A.M., and van Velthoven, P.J., "Comparison of ECMWF analysis and forecast humidity data with CARIBIC upper troposphere and lower stratosphere observations," *Q. J. R. Meteorol. Soc.*, Vol. 141A, No. 688, 2015, pp. 833–844, doi: 10.1002/qj.2400.

[30] Heise, S., Wickert, J., Beyerle, G., Schmidt, T., Smit, H., Cammas, J.-P., and Rothacher, M., "Comparison of water vapor and temperature results from GPS radio occultation aboard CHAMP with MOZAIC aircraft measurements," *IEEE Transact. Geosci. Remote Sens.*, Vol. 46, No. 11, 2008, pp. 3406-3411, doi: 10.1109/TGRS.2008.920268.

[31] Cardinali, C., Isaksen, L., and Anderson, E., "Use and impact of automated aircraft data in a global 4DVAR data assimilation system," *Mon. Wea. Rev.*, Vol. 131, No. 8, 2003, pp. 1865-1877, doi: 10.1175//2569.1.

[32] Dirksen, R.J., Sommer, M., Immler, F.J., Hurst, D.F., Kivi, R., and Vömel, H., "Reference quality upper-air measurements: GRUAN data processing for the Vaisala RS92 radiosonde," *Atmos. Meas. Tech.*, Vol. 7, No. 12, 2014, pp. 4463-4490, doi: 10.5194/amt-7-4463-2014.

[33] Vömel, H., David, D.E., and Smith, K., "Accuracy of tropospheric and stratospheric water vapor measurements by the cryogenic frost point hygrometer: Instrumental details and observations," *J. Geophys. Res.*, Vol. 112, 2007, pp. D08305, doi: 10.1029/2006JD007224.

[34] Immler, F.J., Dykema, J., Gardiner, T., Whiteman, D.N., Thorne, P.W., and Vömel, H., "Reference Quality Upper-Air Measurements: guidance for developing GRUAN data products," *Atmos. Meas. Tech.*, Vol. 3, 2010, pp. 1217-1231, doi: 10.5194/amt-3-1217-2010.

[35] Bodeker, G.E., Bojinski, S., Cimini, D., Dirksen, R.J., Haeffelin, M., Hannigan, J.W., Hurst, D.F., Leblanc, T., Madonna, F., Maturilli, M., Mikalsen, A.C., Philipona, R., Reale, T., Seidel, D.J., Tan, D.G.H., Thorne, P.W., Vömel, H., and Wang, J., "Reference Upper-Air Observations for climate - from concept to reality," *Bull. Amer. Meteorol. Soc.*, Vol. 97, No. 1, 2016, pp. 123-135, doi: 10.1175/BAMS-D-14-00072.1.